Electronic Supplementary Material (ESI) for Nanoscale.

Supporting Information

Aerogel Materials with Periodic Structures Imprinted with Cellulose Nanocrystals

Yi-Tao Xu,[a] Yiling Dai,[a] Thanh-Dinh Nguyen,[a] Wadood Y. Hamad,[b] and Mark J. MacLachlan[a,*]

[a]Department of Chemistry, University of British Columbia, 2036 Main Mall, Vancouver, British Columbia, V6T 1Z1, Canada.

[b]FPInnovations, 2665 East Mall, Vancouver, British Columbia, V6T 1Z4, Canada.

*Email: mmaclach@chem.ubc.ca

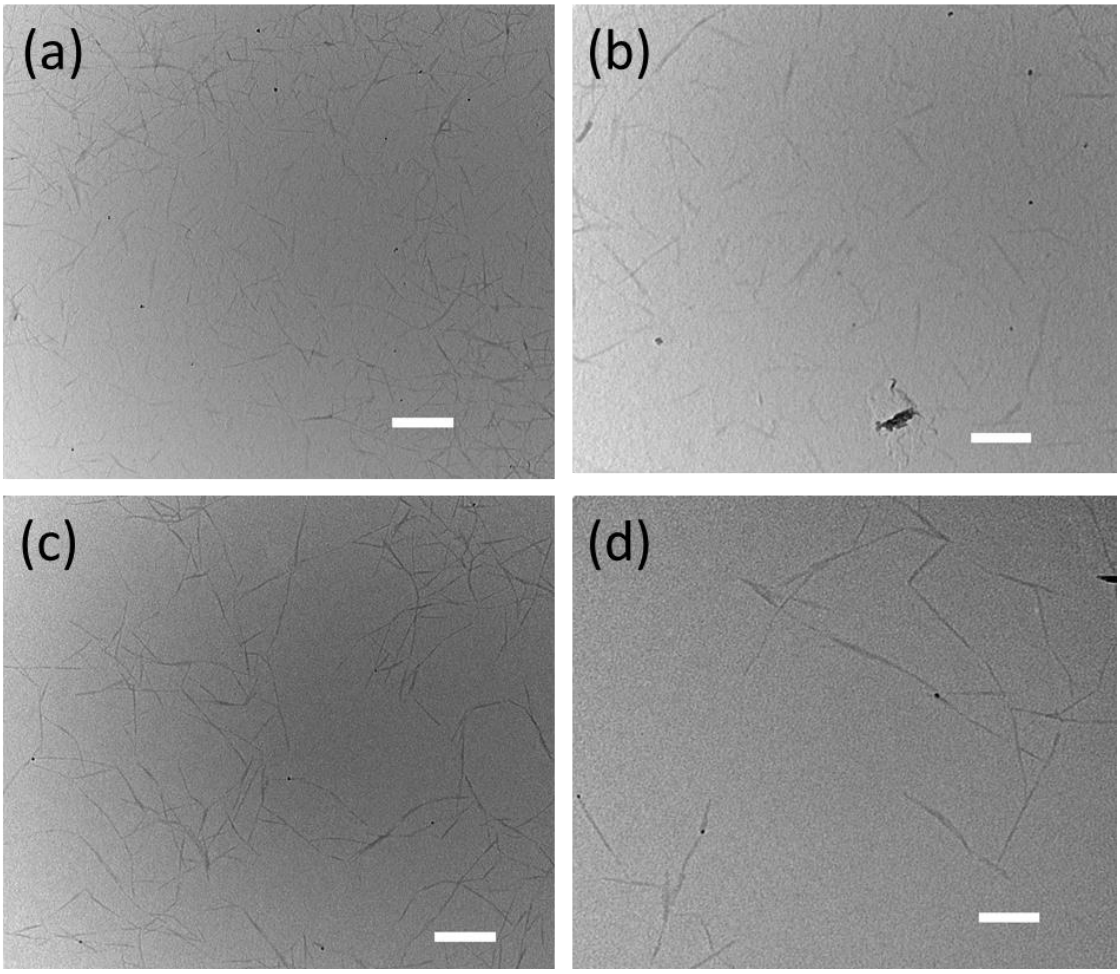

Fig. S1 TEM image of cellulose nanocrystals (CNC-H) from (a and b) upper phase CNC suspension; (c and d) lower phase CNC suspension. (scale bars: 400 nm for a and c; 200 nm for b and d)

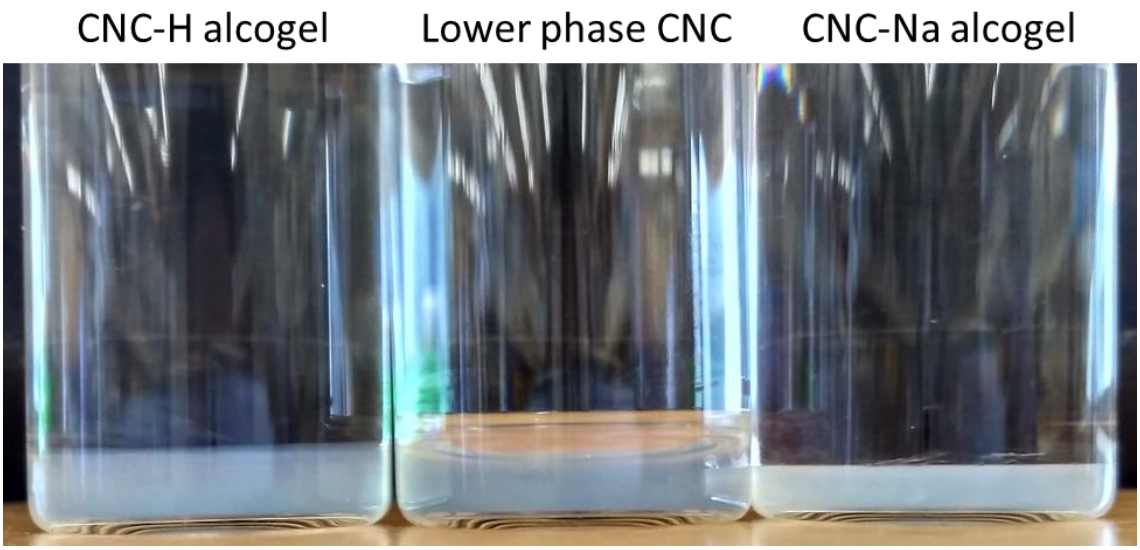

Fig. S2 Digital image of a CNC alcogel and the corresponding CNC suspension (2 mL). The CNC-Na alcogel displays larger shrinkage than CNC-H.

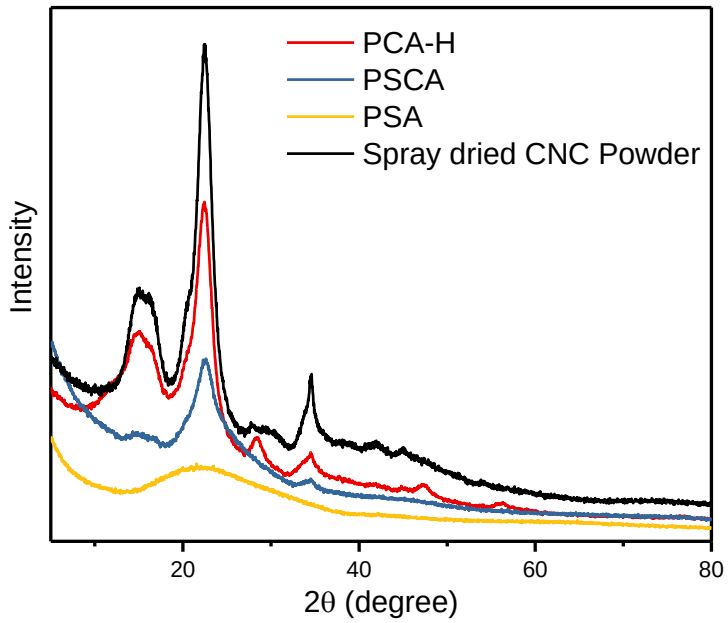

Fig. S3 Powder X-ray diffraction (PXRD) patterns of cellulose (PCA-H), cellulose/silica (PSCA-50), silica (PSA-50) aerogels and the commercial spray dried CNC powders. PXRD patterns of PCA-H, spray dried CNC powders and PSCA-50 display two peaks characteristic of crystalline cellulose around $2\theta \approx 15.2°$ and 22.5°. PXRD of PSA-50 shows only a broad peak characteristic of amorphous silica and no peaks associated with the CNCs.

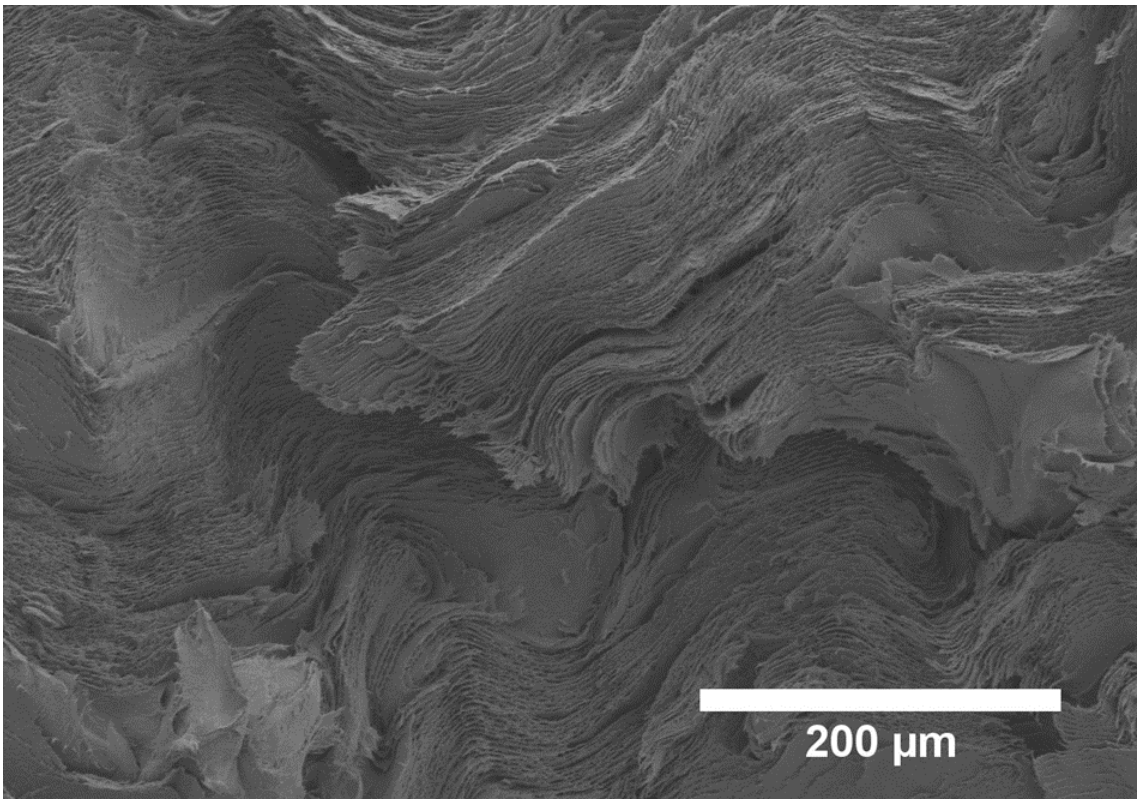

Fig. S4 SEM image of a cross-section of **PCA-Na** shows the pervasive layered structure of the material.

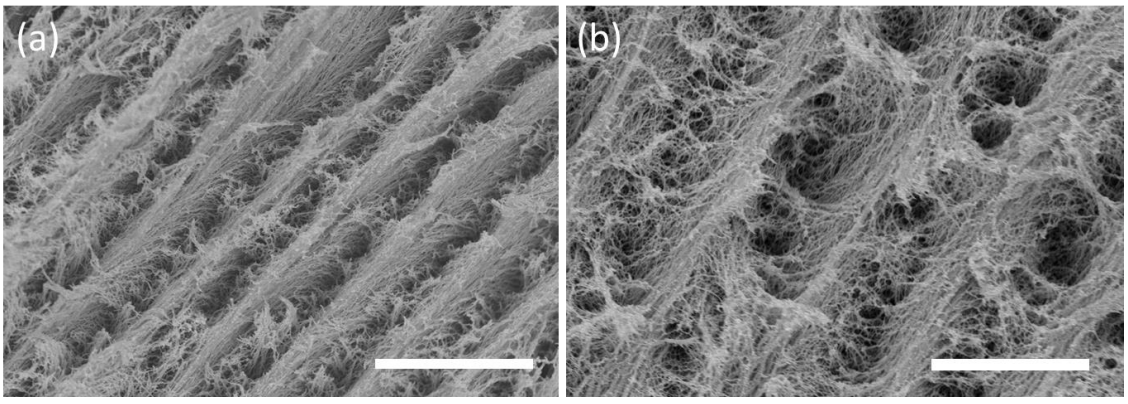

Fig. S5 SEM images of cross sections of (a) **PCA-Na** and (b) **PCA-H**. Scale bars: 5 µm

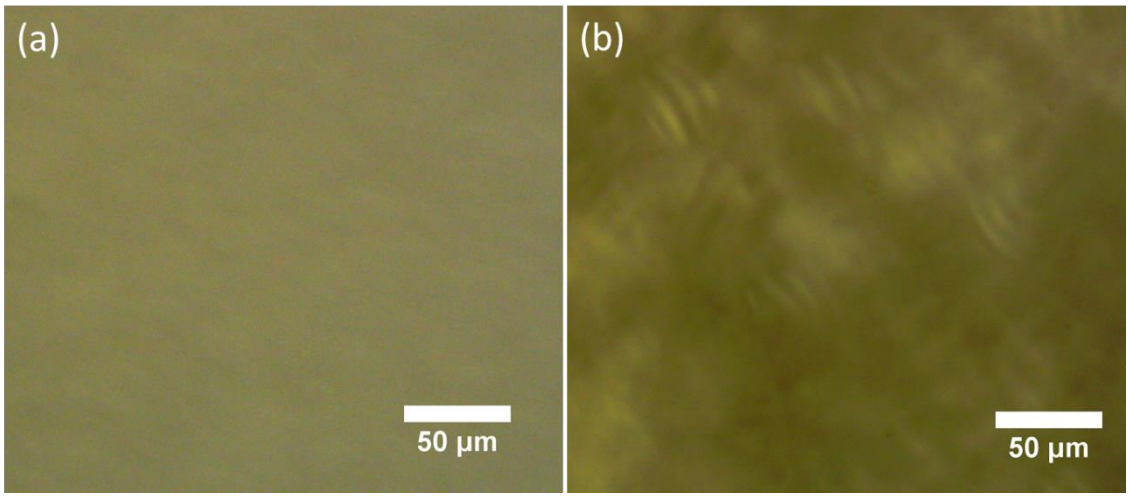

Fig. S6. POM image of 1.7 wt% CNC-Na suspension before (a) and after gelation (b)

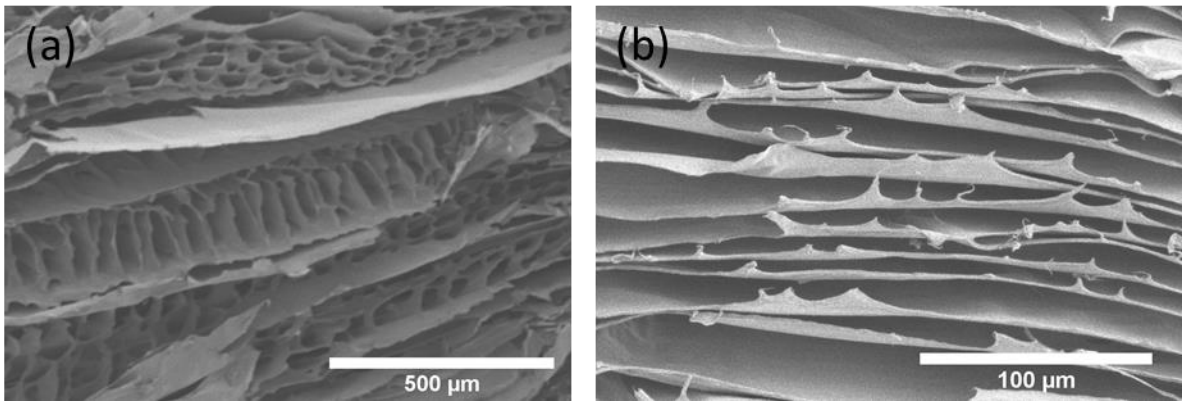

Fig. S7 (a,b) SEM images of the cross section of a cellulose cryogel prepared from the lower phase CNCs.

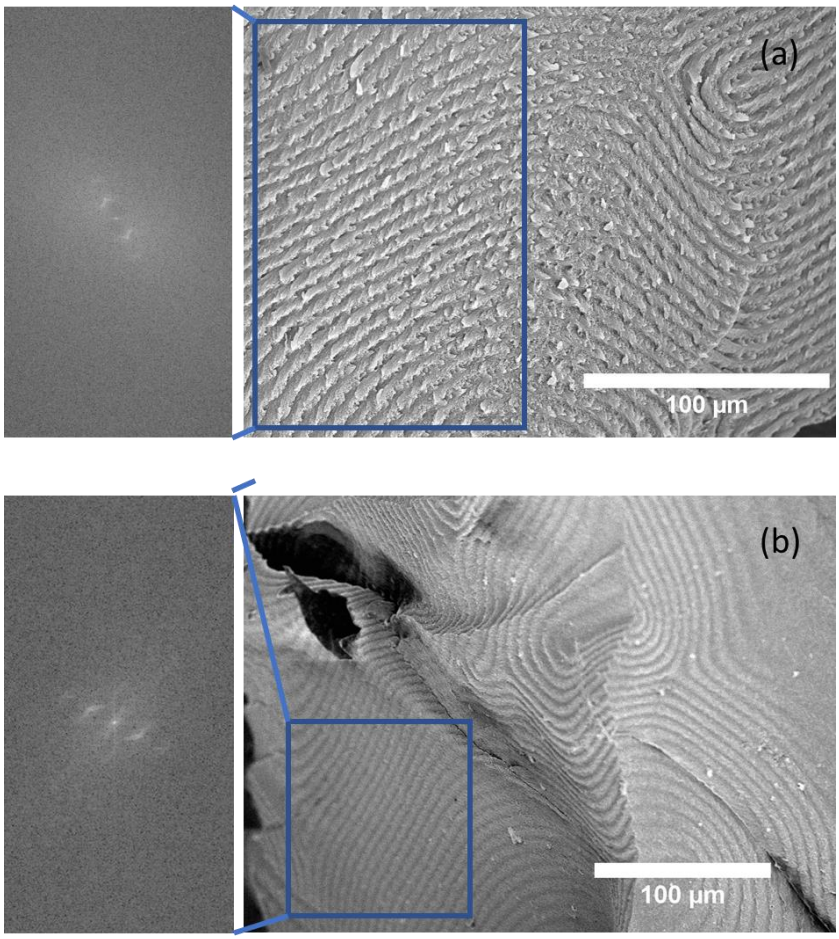

Fig. S8 SEM image of a cross-sections of (a) PSCA-70 and (b) PSA-70, as well as their corresponding fast Fourier-transform patterns.

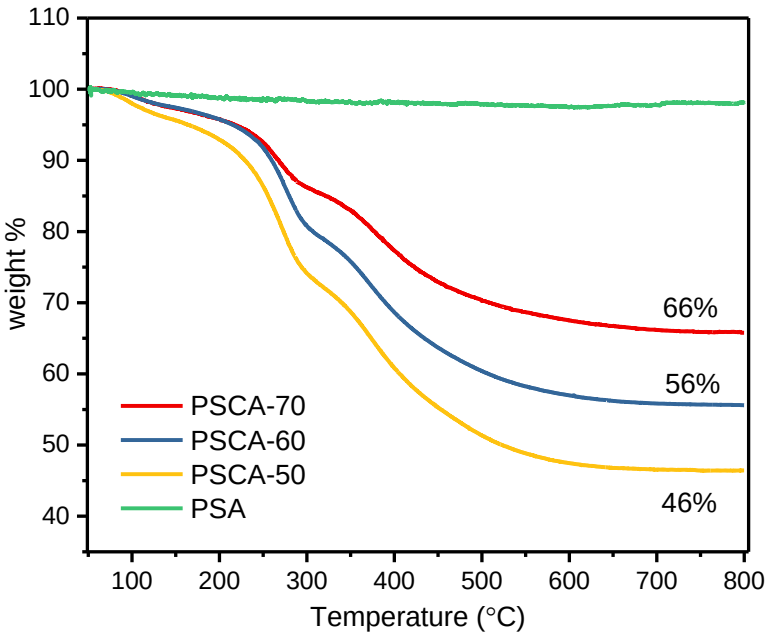

Fig. S9 Thermogravimetric analysis (TGA, 10 °C/min heating rate, under air atmosphere) of periodic silica/cellulose aerogel (PSCA) and silica-only aerogel (PSA) under air. From the TGA, the silica loading was determined to be ca. 46%, 56%, and 66% for PSCA-50, PSCA-60 and PSCA-70, respectively.

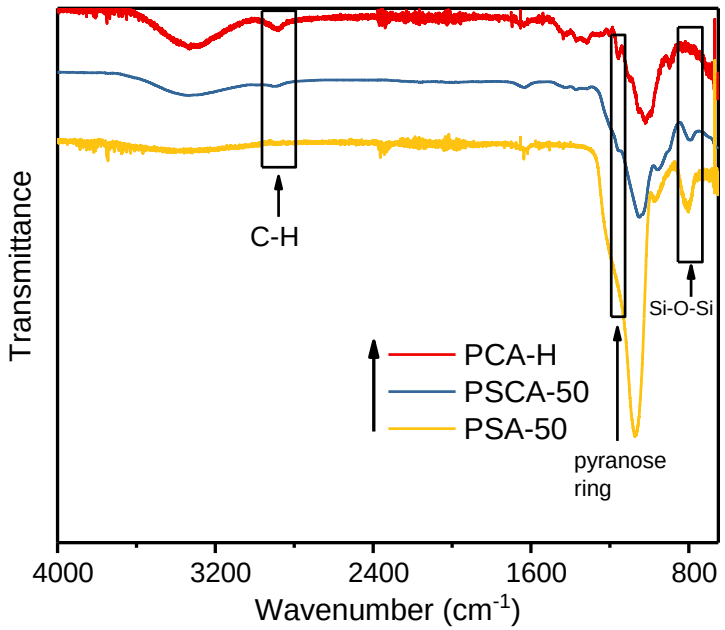

Fig. S10 FTIR spectra for PCA-H, PSCA-50 and PSA-50 (The arrows point out the characteristic peak of CNC and silica).

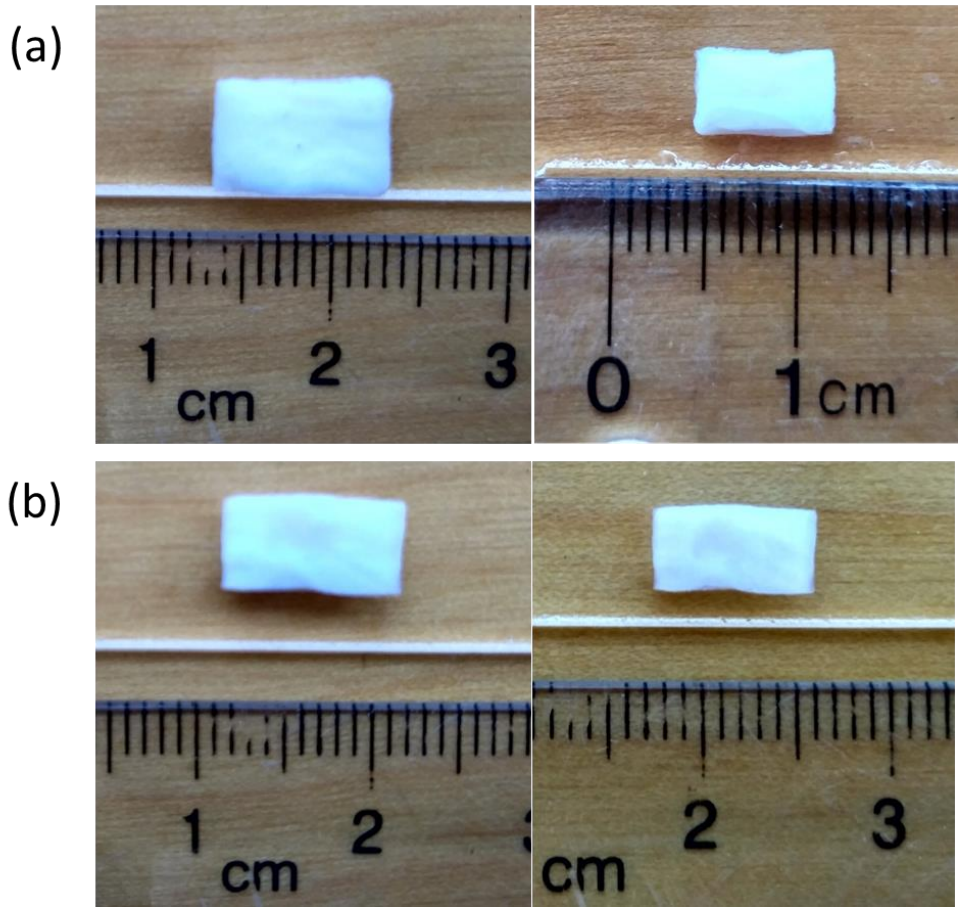

Fig. S11 Digital images of periodic cellulose/silica aerogel before and after calcination for (a) **PCSA-50** and (b) **PCSA-60** with silica loadings of 50% and 60%, respectively.

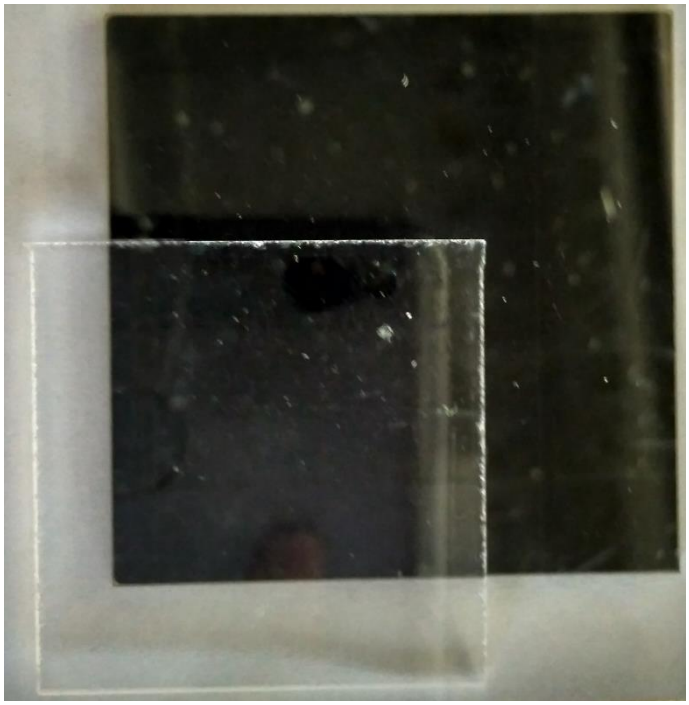

Fig. S12 Photograph of commercial quartz plate between cross polarizers as a control.

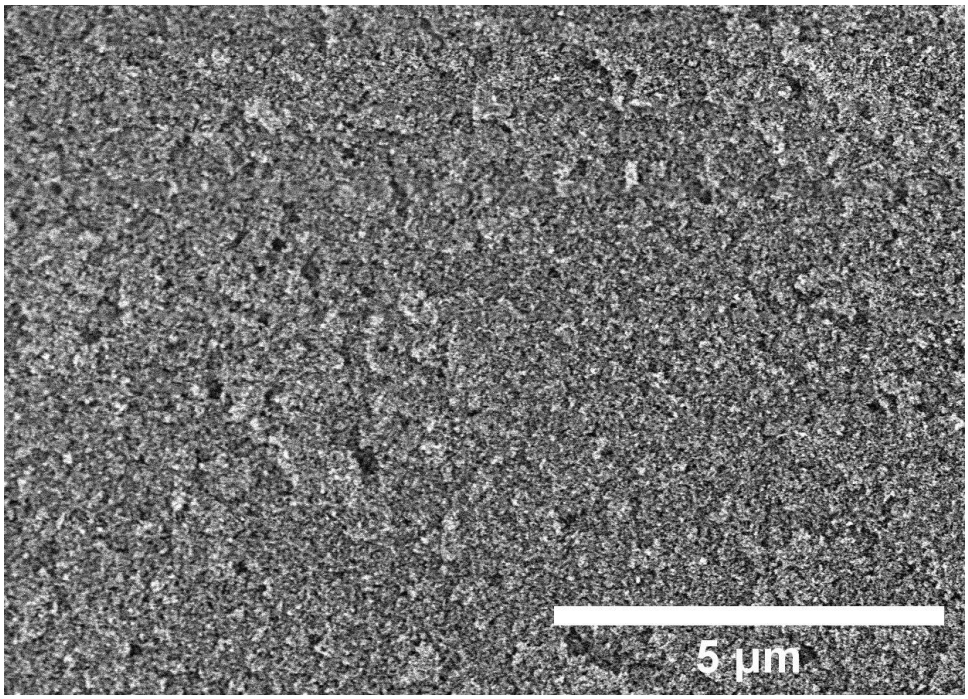

Fig. S13 SEM image showing a cross-section of the two-step catalyzed silica aerogel (**SiO_2-B**, hydrolysis under acidic conditions and then condensation under basic conditions).

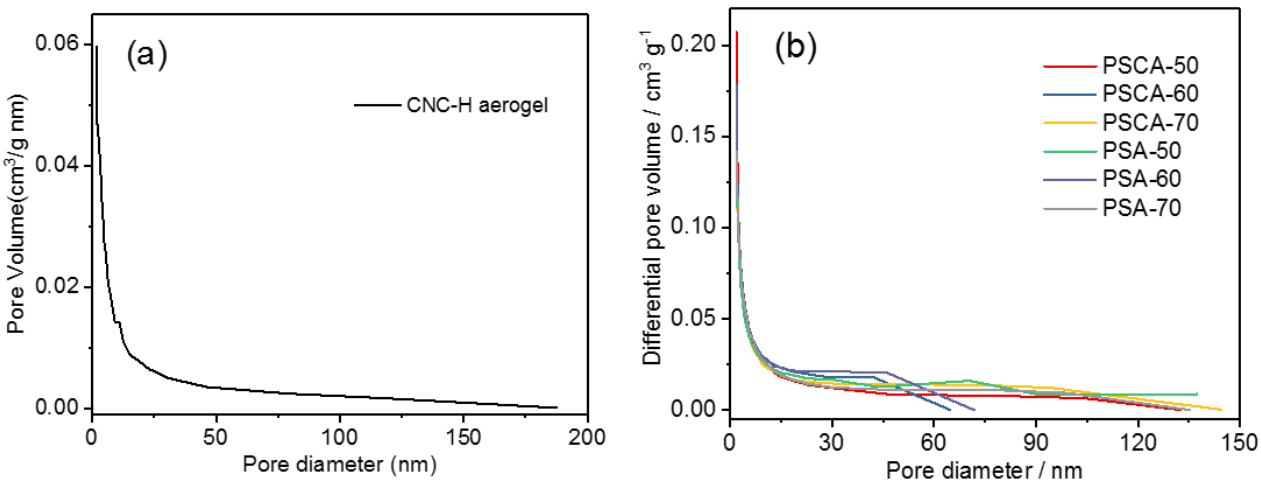

Fig. S14 Pore size distributions of (a) CNC-H aerogel. (b) cellulose/silica and pure silica aerogel. Distributions were determined from the adsorption branch of the isotherm

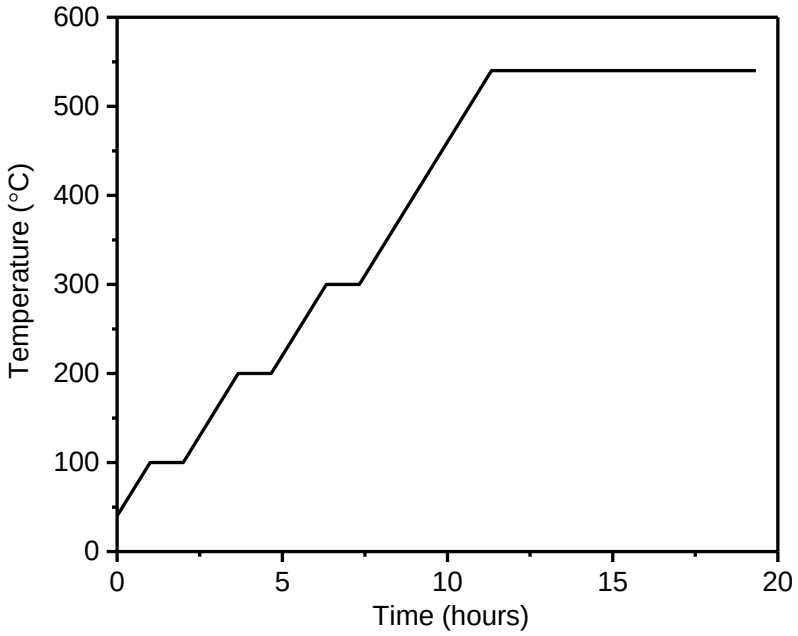

Fig. S15 Temperature program for the calcination experiments.

Table S2. Pore volume for different pore size ranges

Sample	V_{mi} ($cm^3\ g^{-1}$)	V_{me} ($cm^3\ g^{-1}$)	Vp (cm^3 g-1) (pores between 1.7nm and 300 nm)	V_T ($cm^3\ g^{-1}$)	100 V_{me}/V_T %
PCA-H	0.01	0.51	0.79	17.46	2.92
PCA-Na	0.01	0.47	0.74	13.40	3.51
PSCA-50	0.06	1.18	1.59	8.22	14.36
PSCA-60	0.04	1.41	1.56	4.25	33.17
PSCA-70	0.04	1.30	2.42	3.91	33.23
PSA-50	0.03	1.22	2.33	8.17	14.93
PSA-60	0.03	1.71	1.90	6.46	26.47
PSA-70	0.02	1.89	1.89	6.14	30.77

Note: micropore volume (V_{mi}), mesopore volume (V_{me}), the BJH cumulative pore volume (pore between 1.7 nm and 300 nm) (V_P) and the total pore volume (V_T). The Calculation for the total pore volume are based on the following equation:

$$V_T = \frac{1}{\rho} - \frac{1}{\rho_{skeleton}}$$

$$\rho_{skeleton} = \frac{1}{\frac{\omega_s}{\rho_s} + \frac{\omega_c}{\rho_c}}$$